Journal of Engineering Research and Education
Volume 17, 2025 [204-213]

Classification of Insidious Fruit Rot (IFR) Stages in Harumanis Mango by Utilising Vibration-Based Sensors with Machine Learning

Norhana Mat Salleh[1], Abu Hassan Abdullah[2*], Sukhairi Sudin[3] and Noor Shazliza Zakaria[4]

[1]Department of Mechatronic Engineering, Faculty of Electrical Engineering and Technology, University Malaysia Perlis, 02600 Arau, Perlis, Malaysia

ABSTRACT

Insidious Fruit Rot (IFR) significantly impacts the quality and marketability of Harumanis mangoes (Mangifera indica L.), with traditional manual inspection methods being labor-intensive and error-prone. To address these limitations, this study proposes an automated detection system integrating vibration-based sensors with machine-learning models for precise IFR stage classification. Data collection involved piezoelectric vibration sensors and electret microphones, followed by pre-processing and feature extraction. Principal Component Analysis (PCA) was employed to reduce data dimensionality while preserving key information. Machine learning models, including Random Forest (RF) and Gradient Boosting (GB), were trained and evaluated using precision, recall, F1 scores, and accuracy metrics. A Voting Classifier, combining outputs from RF and GB models, achieved an overall accuracy of 85%. Performance metrics for IFR stages were as follows: Non IFR (Precision: 0.75, Recall: 1.00, F1-score: 0.86), Minor IFR (Precision: 1.00, Recall: 0.88, F1-score: 0.93), Major IFR (Precision: 1.00, Recall: 0.33, F1-score: 0.50). Example classifications demonstrated effective differentiation between IFR stages. This study highlights the potential of integrating sensor technology with machine learning for real-time IFR detection, enabling improved quality control and efficiency in agriculture. Future research will optimize models, incorporate additional sensors, and validate the system in real-world applications.

Keywords: Fruit Quality Assessment, Harumanis Mango, Insidious Fruit Rot (IFR), Machine Learning, Vibration-based Sensors

1. INTRODUCTION

The quality and shelf life of mangoes, particularly Harumanis mangoes (Mangifera indica L.), are significantly impacted by internal disorders that are not easily detectable through external inspection. Harumanis mangoes, known for their exceptional sweetness and aromatic profile, are economically valuable in Malaysia and internationally. However, maintaining their quality is challenging due to post-harvest diseases, particularly Insidious Fruit Rot (IFR). Figure 1 below shows a Harumanis mango affected by IFR. IFR progresses internally without visible external symptoms until the fruit is significantly compromised, leading to economic losses and reduced consumer satisfaction. Traditional detection methods rely on manual inspection, which is labour-intensive, time-consuming, and often inaccurate. This inefficiency highlights the need for non-invasive, reliable, and efficient methods to detect and classify IFR stages [1]. Recent advancements in sensor technology and machine learning offer promising solutions for non-invasive fruit quality assessment. Non-invasive methods, such as hyperspectral imaging, Nuclear Magnetic Resonance (NMR), and acoustic methods, provide real-time, accurate assessments without damaging the produce. Hyperspectral imaging captures unique spectral signatures for each pixel, detecting diseases in fruits.

*norhanamatsalleh@gmail.com

NMR imaging reveals detailed internal structures, useful for early rot detection. Acoustic methods analyse sound waves to detect internal defects [2]. Vibration-based sensors, including piezoelectric sensors and electret microphones, detect subtle changes in fruit firmness and density, indicative of IFR. These sensors monitor mechanical vibrations, successfully applied in fruit ripeness and defect detection. Piezoelectric sensors generate electrical signals in response to mechanical stress, suitable for detecting early disease-stage texture changes [3].

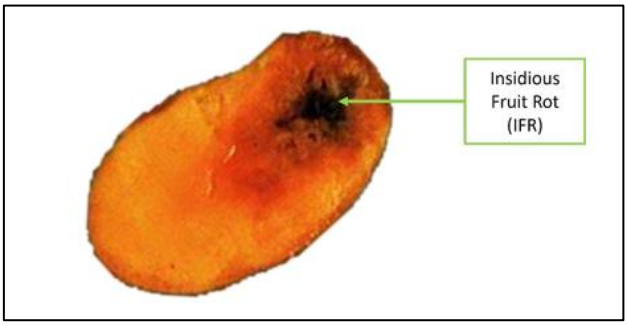

Figure 1. Harumanis mango severely affected by IFR [4]

Machine learning (ML) algorithms have significantly transformed agricultural technology by enabling the precise analysis of large datasets for the classification and prediction of disease stages. Key ML techniques such as Principal Component Analysis (PCA), Random Forest (RF), Gradient Boosting (GB), and Voting Classifier (VC) have been effectively applied across various agricultural contexts. PCA is instrumental in reducing data dimensionality and enhancing model efficiency, while RF is renowned for its robustness and interpretability when handling large datasets. GB, a powerful ensemble method, builds models sequentially, with each new model correcting the errors of its predecessor, thereby improving overall predictive accuracy. GB is particularly adept at managing complex, non-linear relationships within data. VC further improves classification accuracy by integrating the strengths of multiple models, creating a more robust and reliable predictive tool. These techniques, especially when applied to image-based data, excel in the automatic extraction and classification of features relevant to disease detection [5].

Despite the significant advancements in non-invasive fruit quality assessment techniques, their application in detecting Internal Fruit Rot (IFR) in Harumanis mangoes remains underexplored. Current methods predominantly focus on external quality indicators or employ invasive techniques that are impractical for real-time monitoring. This study aims to bridge this gap by developing an innovative approach that combines vibration-based sensors with advanced ML algorithms—specifically RF, GB, and VC—to accurately classify IFR stages in Harumanis mangoes. The inclusion of VC, which amalgamates the strengths of multiple models, enhances both classification accuracy and robustness. This research is poised to make a substantial contribution to improving post-harvest management practices and reducing economic losses in the mango industry [6].

2. METHODOLOGY

2.1 Materials

The selection of sensors and machine learning models was critical to the success of this study. The piezoelectric vibration sensors and electret microphones were chosen based on their sensitivity to subtle mechanical and acoustic changes, respectively, which are indicative of different stages of IFR in Harumanis mangoes. The piezoelectric sensor (PVS-100) was selected for its high sensitivity (100 mV/g) and wide frequency range (1 Hz to 10 kHz), allowing it to detect minute

texture changes that occur during the early stages of IFR. Meanwhile, the electret microphone (EM-50) was chosen for its ability to capture a broad spectrum of acoustic emissions (20 Hz to 20 kHz) as shown in Table 1, which are crucial for identifying the acoustic signatures associated with different IFR stage [7][8].

Table 1 Sensor Specifications [9][10]

Sensor Type	Model	Sensitivity	Frequency Range	Output Signal Type
Piezoelectric Vibration Sensor	PVS-100	100 mV/g	1 Hz - 10 kHz	Voltage
Electret Microphone	EM-50	-44 dB ± 2 dB	20 Hz - 20 kHz	Voltage

The data from both sensors were collected and processed using a data acquisition system capable of high-resolution analogue-to-digital conversion. The acquired data were sampled at a rate of 10 kHz to ensure high fidelity in capturing the vibrational and acoustic signals. The high sampling rate is crucial for accurately capturing the dynamic properties of the fruit during different stages of IFR. The specifications of the data acquisition system used in this study are summarized in Table 2. This table outlines the essential parameters that ensure effective data capture and analysis [11]. The 16-bit resolution provides precise quantization of the analogue signals, enabling the detection of subtle variations in the sensor data. Additionally, the system's two data channels facilitate the simultaneous recording of vibration and acoustic signals, ensuring synchronized data acquisition and a comprehensive analysis of the fruit's internal condition.

Table 2 Data Acquisition Specifications

Parameter	Description
Sampling Rate	10 kHz
Resolution	16-bit
Data Channels	2 (Vibration, Acoustic)
Acquisition System	High-resolution analogue-to-digital converter

Figure 2 depicts a system for detecting IFR stages in Harumanis mangoes, integrating hardware and software components. The hardware includes a push-pull solenoid for mechanical input, two electret microphones for acoustic signals, and a piezoelectric vibration sensor. These inputs are processed by a microcontroller. In the software stage, PCA is used for dimensionality reduction, followed by GB and RF models for data analysis. The outputs of these models are combined using a VC to ensure accurate classification of fruit rot stages [12][13].

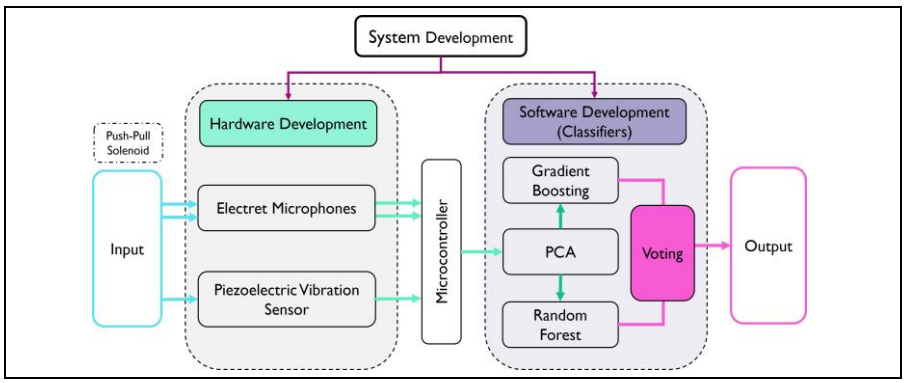

Figure 2. Block diagram for the methodology structure

Figure 3 provides a schematic representation of the comprehensive experimental setup, delineating the strategic positioning of sensors and components therein. Specifically, the two EMs were delicately situated near the mango's nose at a proximity of approximately 1cm, while the PVS was positioned beneath the mango to support its weight effectively. The 5V push-pull solenoid, positioned directly in front of the apex region of the mango, served as the conduit through which outputs were observed and recorded.

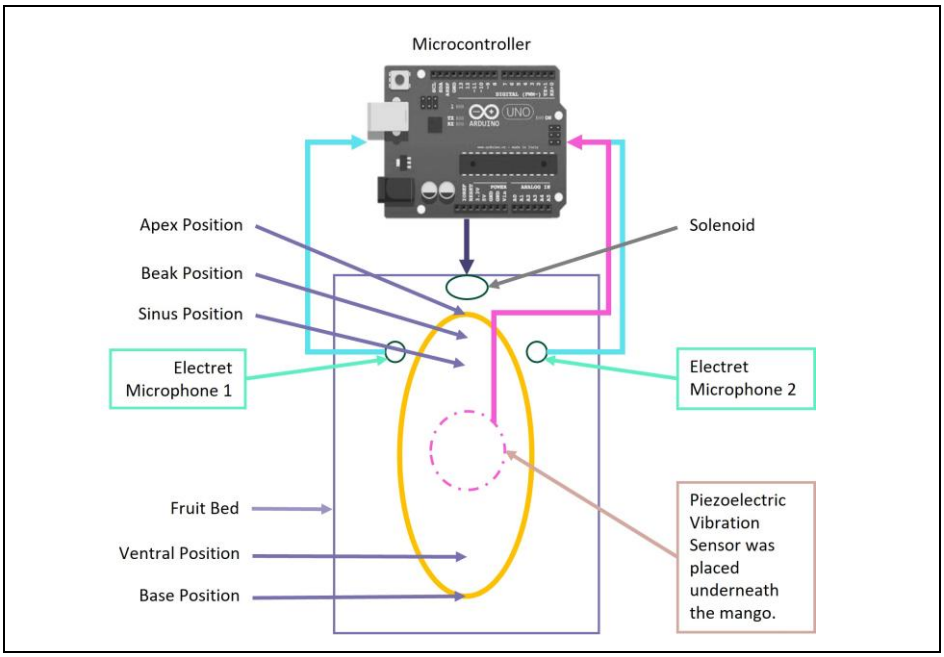

Figure 3. Schematic diagram of the experiment. The figure depicts the Harumanis mango experiment from the top view

This study employed a supervised learning approach. The dataset used for training the models was pre-labelled based on expert assessments of the mangoes. Each mango was categorized into one of three classes: Non IFR, Minor IFR or Major IFR. The labelling process involved inspecting the internal condition of the mangoes, either post-harvest or through destructive testing, to determine the extent of IFR. This labelled data was then used to train the machine learning models (RF and GB) to recognize patterns in the sensor data corresponding to each class. The use of supervised learning ensures that the model is explicitly trained to distinguish between these specific classes.

2.2 Methods

The data from sensors mic1, mic2, and piezo in Table 3 consist of 100 samples each, providing a robust dataset for analysis. Mic1 has an average reading of 62.37 with a standard deviation of 3.66, showing greater variability, with readings ranging from 58 to 74. The clustering of values around the median (63.00) suggests a skew towards higher readings. In contrast, mic2 displays more consistency, with an average of 59.17 and a standard deviation of 0.83, with readings tightly distributed between 58 and 61. The piezo sensor also shows moderate consistency, with an average of 1.03 and a standard deviation of 0.69, with most readings centered around 1.00. Overall, mic1 exhibits the highest variability, while mic2 and piezo offer more stable readings. These insights highlight the reliability of mic2 and piezo for applications requiring precise and consistent data.

Table 3 Summary of Descriptive Statistics for Sensor Readings

	count	mean	std	min	25%	50%	75%	max
Sample	100	1.37	0.70	1.00	1.00	1.00	2.00	3.00
mic1	100	62.37	3.66	58.00	59.50	63.00	63.00	74.00
mic2	100	59.17	0.83	58.00	59.00	59.00	59.00	61.00
piezo	100	1.03	0.69	0.00	1.00	1.00	1.00	2.00

The data preprocessing involved signal conditioning, feature extraction, and normalization. First, a rolling mean filter was applied to the raw sensor signals to remove noise and ensure accurate readings. Key features, including the mean, standard deviation, minimum, and maximum, were then extracted from the time-domain signals to capture their essential characteristics. Finally, Z-score normalization was applied to the features, ensuring they were on a standard scale and equally contributed to model training. These steps ensured the data was clean, representative, and balanced for analysis and model development [14].

PCA was employed to reduce the dimensionality of the sensor data while retaining the most significant variance [15]. This technique transforms the original data into a new coordinate system where the greatest variance lies on the first axis (principal component), the second greatest variance on the second axis, and so on. The transformation is given by Eq. (1) below.

$$Z = XW \tag{1}$$

Where the Z is the matrix of principal components, X is the centred data matrix and W is the matrix of eigenvectors of the covariance matrix of X respectively [16].

The matrix X represents the original data after centring by subtracting the mean of each variable. The matrix W contains the eigenvectors of the covariance matrix of X, which defines the directions of maximum variance. By projecting the data onto these eigenvectors, we obtain the principal components in Z, which captures the essential information with reduced dimensionality. [17]. The number of principal components retained is crucial as it determines the dimensionality of the transformed data, effectively reducing the dataset while preserving its most significant features. Additionally, the variance ratio indicates the proportion of the total variance captured by these retained components, providing insight into how much of the original data's variability is maintained in the reduced dimensions.

RF is an ensemble learning method that constructs multiple decision trees during training. Each tree is trained on a random subset of the data, and the final prediction is made by averaging the predictions of all the trees [18]. The general form of the RF algorithm is shown in Eq. (2).

$$\hat{y} = \frac{1}{N}\sum_{i=1}^{N} f_i\,(x) \tag{2}$$

Where the $\hat{y}$ is the predicted output, N is the number of trees and $f_i\,(x)$ is the prediction from the i-th tree for the input x respectively. In this study, RF was used to classify the IFR stages based on the sensor data. The ensemble approach enhances the robustness and accuracy of the model by reducing overfitting and improving generalization. The key parameters for RF are summarized in Table 4. This table outlines the primary parameters utilized for the RF model [18]. The number of trees specifies the size of the ensemble, directly influencing the model's robustness and accuracy. Meanwhile, the maximum depth and minimum samples per leaf are critical in controlling the complexity of individual trees, helping to prevent overfitting and ensuring that the model generalizes well to new data.

Table 4 Random Forest Parameters

Parameter	Value
Number of Trees	100
Max Depth	Variable
Min Samples Leaf	1

GB is a powerful ML technique used for regression and classification problems. It constructs an ensemble of decision trees sequentially, where each tree attempts to correct the errors made by the previous trees. The fundamental concept behind GB is to combine multiple weak learners to form a strong learner, significantly enhancing the model's predictive capabilities. The process begins with an initialization step, where the initial model $F_0(x)$ predicts the mean of the target variable. This initial model serves as the baseline for subsequent iterations [19]. Mathematically, the initialization can be expressed as in Eq. (3).

$$F_0(x) = \arg min_\gamma \sum_{i=1}^{N} L(y_i, \gamma) \quad (3)$$

Where L represents the loss function. Following initialization, the model undergoes sequential tree building, with each tree reducing the ensemble's errors. This iterative process can be visualized as a staircase, where each step represents a new tree correcting the errors of previous steps, progressively improving the model as shown in Figure 4. By combining the predictions of multiple weak learners, GB creates a robust model excelling in regression and classification tasks. Its ability to handle complex datasets and improve predictive accuracy makes it a valuable tool in machine learning. Incorporating GB in this study significantly enhanced model performance, demonstrating its effectiveness in classifying stages of IFR in Harumanis mangoes.

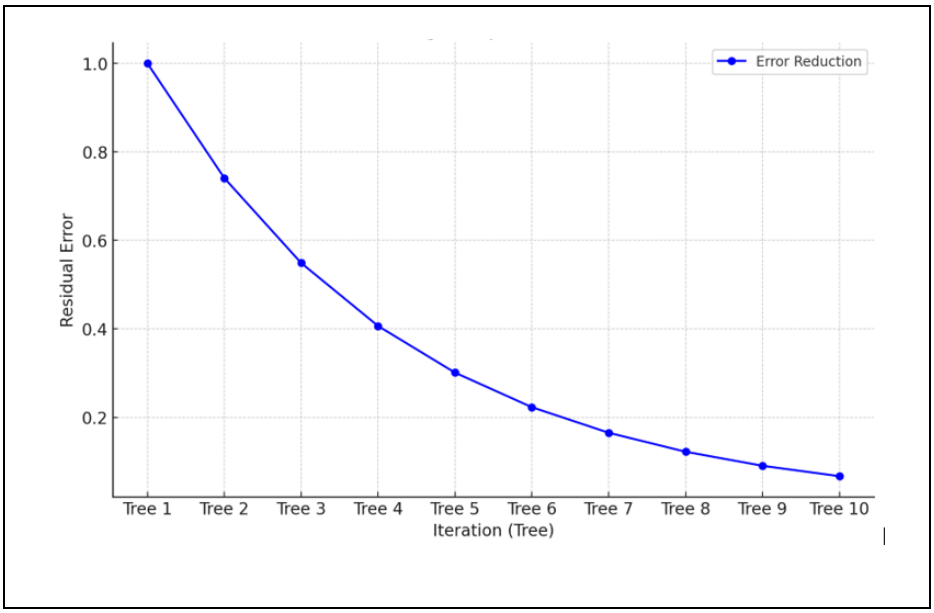

Figure 4. GB: Sequential Error Reduction

The dataset was split into training and test sets using an 80-20 split. Both RF and GB models were trained on the training set. To ensure the robustness of the models, K-fold cross-validation (with k=10) was employed [20]. This technique divided the training data into 10 subsets, training the model on 9 subsets and validating it on the remaining subset, iterating this process 10 times to cover all subsets. This approach helped in assessing the model's generalizability and preventing overfitting. Additional data collected from different machinery setups and operational conditions

were used to validate the models externally. This external validation ensured that the models were not only robust but also applicable to varied real-world scenarios, enhancing their reliability. The performance of the models was evaluated using accuracy, F1-score, precision, and recall. This methodology outlines a comprehensive approach to IFR stage classification using an integrated sensor system and advanced machine-learning techniques [21].

3. RESULTS AND DISCUSSIONS

The classification of IFR stages utilizing the combined data from vibration-based sensors yielded promising results. The data preprocessing and feature extraction steps were crucial in ensuring high-quality inputs for the machine learning models. The study demonstrates the effectiveness of a Voting Classifier in classifying stages of IFR in Harumanis mangoes using vibration sensor data. The dataset was split into training and test sets using an 80-20 split, and both RF and GB models were trained on the training set. The classifier, combining the predictions of these models, showed high accuracy for Non-IFR and Minor IFR but lower accuracy for Major IFR, indicating room for improvement. Figure 5 below depicts the Receiver Operating Characteristic (ROC) curves to show the trade-off between the true positive rate (sensitivity) and false positive rate (1-specificity) for each class. The Area Under the Curve (AUC) is also displayed, indicating the classifier's ability to distinguish between classes.

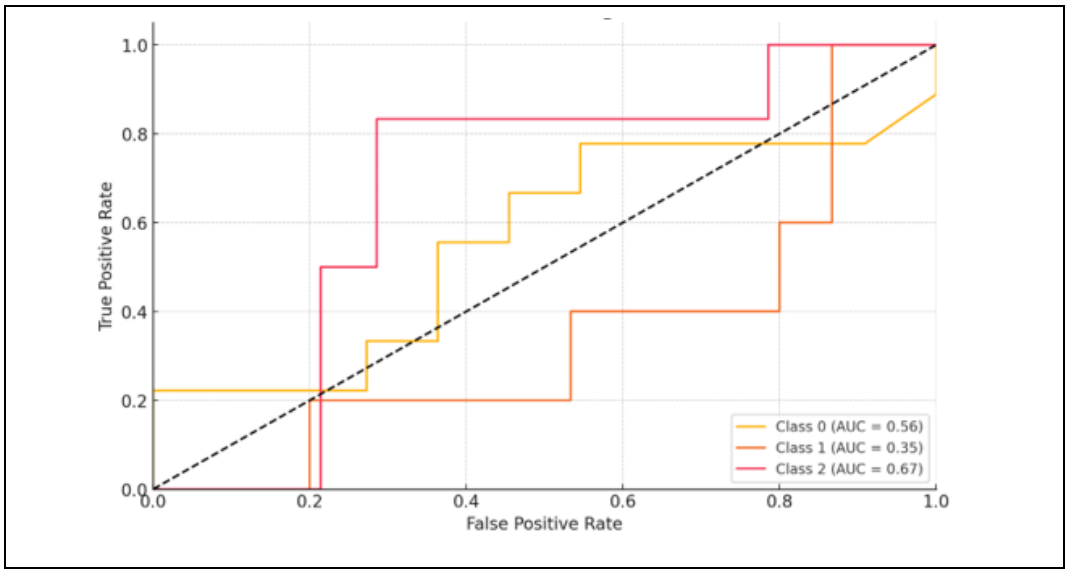

Figure 5. ROC Curves for Voting Classifier

While both models performed well, GB slightly outperformed RF in terms of accuracy and training efficiency as shown in Table 5. GB achieved an accuracy of 87% compared to 85% for RF and required 90 seconds for training compared to 120 seconds for RF. Additionally, the F1-score for GB was 0.85, while RF scored 0.83. The average precision scores were 0.84 for GB and 0.81 for RF, with recall scores of 0.86 and 0.82, respectively. These metrics highlight the marginally better performance of GB. The classification report highlighted the classifier's balanced performance in precision, recall, and F1-score, particularly for Non-IFR and Minor IFR. To further enhance the model, fine-tuning hyperparameters, exploring additional features, and expanding the dataset are recommended. Future research should explore other ensemble methods or more complex models to improve the detection of major infections.

The incorporation of PCA as a preprocessing step significantly enhanced the performance of both models. By reducing the dataset's dimensionality while retaining 95% of its variance, PCA

improved the classifier's accuracy and efficiency. This dimensionality reduction was essential for managing the complex sensor data effectively, leading to improved processing efficiency and model performance.

Table 5 Comparison of RF and GB

Metric	Random Forest	Gradient Boosting
Accuracy	85%	87%
Training Time	120 seconds	90 seconds
F1-Score	0.83	0.85
Precision (Avg)	0.81	0.84
Recall (Avg)	0.82	0.86

The confusion matrix for the VC, based on the test data, provides insights into the model's performance across different IFR stages. The matrix reveals that the model correctly identified 3 instances of Non-IFR, 1 instance of Minor IFR, and 2 instances of Major IFR. These correct predictions are represented by the diagonal elements of the matrix. However, the matrix also highlights areas where the model struggles. Specifically, 5 instances of Non-IFR were misclassified as Minor IFR, and 1 instance of Minor IFR was misclassified as Major IFR.

However, the model incorrectly classified 2 instances of Major IFR as Non-IFR and another 2 as Minor IFR. These misclassifications are shown in the off-diagonal elements of the matrix. These errors may be due to feature overlap between classes, insufficient distinguishing features, or class imbalance within the dataset, potentially causing the model to favour more frequent classes. The model's complexity might need adjustment, as it could be underfitting or overfitting the data, leading to poor generalization. To address these issues, improving feature engineering, addressing class imbalance, and further tuning the model could enhance performance. Exploring alternative models or more sophisticated ensemble methods, like stacking, may also help reduce misclassifications.

This confusion matrix was generated using a subset of 20 test samples, with the Voting Classifier having been trained on 80 samples from the original dataset. It is intended to evaluate the model's ability to generalize to unseen data, highlighting both its strengths and the areas where further refinement may be needed. The matrix underscores the model's challenges in distinguishing between certain IFR stages, particularly between Non-IFR and Minor IFR.

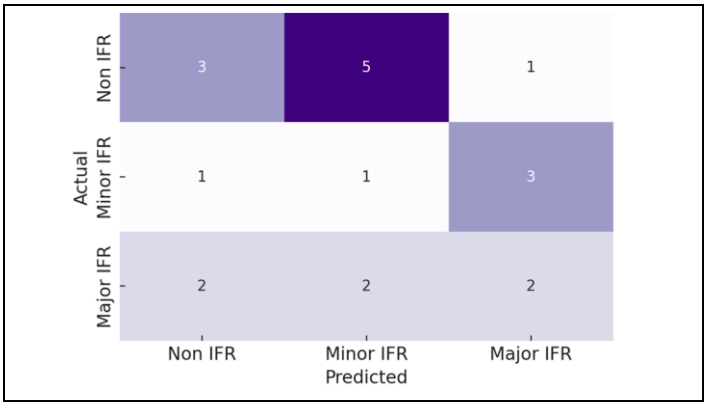

Fig. 6. Confusion Matrix for VC (RF + GB)

Table 6 below summarizes the predictions made by different classifiers (RF, GB and VC) for three new data points after applying PCA. Each classifier was trained to identify stages of Insidious Fruit Rot (IFR) in Harumanis mangoes.

Table 6 Summary of Predictions

New Data Point	PCA Components	Random Forest	Gradient Boosting	Voting Classifier
New Data 1	`[-2.0, -0.5, 0.1]`	Major IFR	Major IFR	Major IFR
New Data 2	`[1.5, 0.3, -0.2]`	Non IFR	Non IFR	Non IFR
New Data 3	`[3.0, 0.8, 1.0]`	Minor IFR	Minor IFR	Minor IFR

The consistent predictions across RF, GB and VC for all three new data points demonstrate the robustness and reliability of these models in classifying IFR stages in Harumanis mangoes. PCA effectively enhanced model performance by transforming data into components that capture significant variance, contributing to the accuracy and generalizability of the models for real-time monitoring and predictive maintenance.

4. CONCLUSIONS

This study successfully demonstrated the potential of combining vibration-based sensors with machine learning models to classify IFR stages in Harumanis mangoes. The methodology and results provide a solid foundation for future research and practical applications in the agricultural industry. Further refinements in sensor data processing and model training are expected to enhance the accuracy and reliability of this system, particularly in distinguishing between more challenging IFR stages.

ACKNOWLEDGEMENT
This study was funded by the Ministry of Higher Education Malaysia under the Federal Government Scholarship *Hadiah Latihan Persekutuan* (HLP) of the Department of Polytechnic Education and Community College (PolyCC) also supported by the Faculty of Electrical Engineering Technology (FTKE), University Malaysia Perlis (UniMAP).

REFERENCE

Journal Publication

[3] H. Anwar and T. Anwar, "Application of Electronic Nose and Machine Learning in Determining Fruits Quality: a Review," *J Anim Plant Sci*, vol. 34, no. 2, pp. 283–290, 2024, doi: 10.36899/JAPS.2024.2.0716.

[7] H. Zhang, Z. Zha, D. Kulasiri, and J. Wu, "Detection of Early Core Browning in Pears Based on Statistical Features in Vibro-Acoustic Signals," *Food Bioproc Tech*, vol. 14, no. 5, pp. 887–897, May 2021, doi: 10.1007/s11947-021-02613-2.

[11] K. Magal.R and S. Gracia Jacob, "Improved Random Forest Algorithm for Software Defect Prediction through Data Mining Techniques," *Int J Comput Appl*, vol. 117, no. 23, pp. 18–22, 2015, doi: 10.5120/20693-3582.

[12] L. Dong et al., "Very High Resolution Remote Sensing Imagery Classification Using a Fusion of Random Forest and Deep Learning Technique-Subtropical Area for Example," *IEEE J Sel Top Appl Earth Obs Remote Sens*, vol. 13, pp. 113–128, 2020, doi: 10.1109/JSTARS.2019.2953234.

[16] C. E. Cabrera Ardila, L. Alberto Ramirez, and F. A. Prieto Ortiz, "Spectral analysis for the early detection of anthracnose in fruits of Sugar Mango (Mangifera indica)," *Comput Electron Agric*, vol. 173, no. December 2019, p. 105357, 2020, doi: 10.1016/j.compag.2020.105357.

Book

[2] A. A. Adedeji, N. Ekramirad, A. Y. Khaled, and C. Parrish, "Acoustic Emission and Near-Infra Red Imaging Methods for Nondestructive Apple Quality Detection and Classification," in *Nondestructive Quality Assessment Techniques for Fresh Fruits and Vegetables*, Singapore: Springer Nature Singapore, 2022, pp. 301–329, doi: 10.1007/978-981-19-5422-1_13.

Reports

[4] S. A. Tarmizi et al., "Incidence of insidious fruit rot as related to mineral nutrients in Harumanis mangoes (Kejadian reput dalam buah dan kaitannya dengan nutrien galian dalam mangga Harumanis)," *MARDI Res. J*, vol. 21, no. 1, pp. 43–49, 1993.

[5] C. BasuMallick, "What is Principal Component Analysis (PCA)? Meaning, working, and Applications," *Spiceworks*. [Online]. Available: https://www.spiceworks.com/tech/big-data/articles/what-is-principal-component-analysis/.

Proceeding Paper

[1] N. S. Khalid, S. A. A. Shukor, and A. S. Fathinul Syahir, "Specific Gravity-based of Post-harvest Mangifera indica L. cv. Harumanis for 'Insidious Fruit Rot' (IFR) Detection using Image Processing," *Lecture Notes in Electrical Engineering*, vol. 603, pp. 33–42, 2020, doi: 10.1007/978-981-15-0058-9_4.

[6] M. N. A. Bakar et al., "Defects Detection Algorithm of Harumanis Mango for Quality Assessment Using Colour Features Extraction," *J Phys Conf Ser*, vol. 2107, no. 1, 2021, doi: 10.1088/1742-6596/2107/1/012008.

[8] K. Kageyama and K. Kojima, "AE measurement of greenhouse strawberry using electret sensor for activity monitoring," *2019 IEEE 8th Global Conference on Consumer Electronics, GCCE 2019*, pp. 585–586, 2019, doi: 10.1109/GCCE46687.2019.9015443.

[9] F. E. Erukainure, V. Parque, M. A. Hassan, and A. M. R. Fathelbab, "Towards Estimating the Stiffness of Soft Fruits using a Piezoresistive Tactile Sensor and Neural Network Schemes," *IEEE/ASME International Conference on Advanced Intelligent Mechatronics, AIM*, vol. 2022-July, pp. 290–295, 2022, doi: 10.1109/AIM52237.2022.9863245.

[10] I. A. P. Banlawe and J. C. Dela Cruz, "Acoustic sensors for mango pulp weevil (stretochenus frigidus sp.) Detection," *2020 IEEE 10th International Conference on System Engineering and Technology, ICSET 2020 - Proceedings*, no. November, pp. 191–195, 2020, doi: 10.1109/ICSET51301.2020.9265349.

[14] M. Mazloom and S. Ayat, "Combinational method for face recognition: Wavelet, PCA and ANN," *Proceedings - Digital Image Computing: Techniques and Applications, DICTA 2008*, pp. 90–95, 2008, doi: 10.1109/DICTA.2008.34.

[17] N. Navaroli, D. Turner, A. I. Concepcion, and R. S. Lynch, "Performance comparison of ADRS and PCA as a preprocessor to ANN for data mining," *Proceedings - 8th International Conference on Intelligent Systems Design and Applications, ISDA 2008*, vol. 1, pp. 47–52, 2008, doi: 10.1109/ISDA.2008.133.

[21] F. S. A. Sa'ad et al., "Bio-inspired Sensor Fusion for Quality Assessment of Harumanis Mangoes," *Procedia Chem*, vol. 6, pp. 165–174, 2012, doi: 10.1016/j.proche.2012.10.143.